Journal of Catalysis **195,** 20–30 (2000)
doi:10.1006/jcat.2000.2979, available online at http://www.idealibrary.com on IDEAL®

Dehydrogenation of Cyclohexanol on Copper-Containing Catalysts

I. The Influence of the Oxidation State of Copper on the Activity of Copper Sites

V. Z. Fridman[1] and A. A. Davydov[2]

Reflex Inc. (Catalysis Center, Research and Consulting), New York, New York

Received October 21, 1999; revised June 23, 2000; accepted June 23, 2000

The X-ray diffraction, X-ray photoelectron spectroscopy, IR spectroscopy of chemisorbed carbon monoxide and kinetic data have been employed to determine the active sites of copper-containing catalysts of both dehydrogenation of cyclohexanol to cyclohexanone and aromatization of cyclohexanol to phenol. Two kinds of copper active sites of the cyclohexanol dehydrogenation reaction to cyclohexanone have been revealed (monovalent copper and metallic copper), and it has been shown that monovalent copper is significantly more active than metallic copper, and monovalent copper does not catalyze the phenol formation. At the same time, metallic copper can play the role of active sites not only in alcohol dehydrogenation to ketone but also in aromatization of cyclohexanol to phenol.

INTRODUCTION

Industrial catalysts of dehydrogenation of cyclohexanol to cyclohexanone are generally based on copper as an active component of catalytic systems. The commercial Cu–Mg and Cu–Zn–Al catalysts usually are used in the temperature range from 220 to 260°C, and the conversion of cyclohexanol on these catalysts is very close to equilibrium values (50–60%) at the 99% selectivity for cyclohexanone (1). The process of cyclohexanol dehydrogenation includes the complex of consequent-parallel reactions, such as dehydrogenation of cyclohexanol to cyclohexanone (the main reaction), aromatization of cyclohexanol to phenol, dehydration of cyclohexanol to cyclohexene, and condensation of cyclohexanone to cyclohexyldencyclohexanone (the last reactions are the formation of byproducts). The mechanisms of dehydration of cyclohexanol and condensation of cyclohexanone are known and the rates of these reactions can be decreased by the acidity of the catalysts (2, 3), but the mechanisms of the main reaction of ketone synthesis and aromatization of cyclohexanol are not fully understandable.

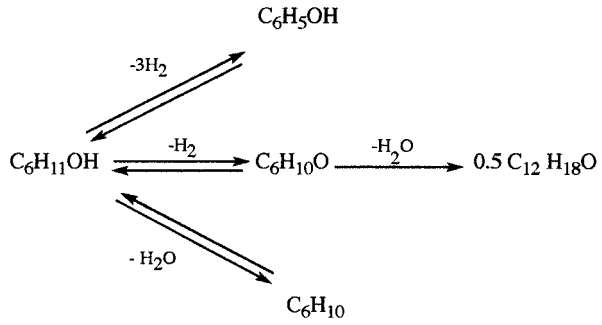

A number of investigations (4–10) have focused on determining the influence of support, of the methods of preparation, and of copper loading on the activity and selectivity of copper-containing catalysts, with the goal of enhancing the conversion of alcohol. Attempts to increase the conversion of cyclohexanol by using new copper catalysts and higher reaction temperatures have not been successful because of a sharp decrease of the selectivity of the process as a result of a sharp increase of the phenol yield in the products of the reaction. The reasons for a decrease in the selectivity of the process and a way to maintain the selectivity of the process for increasing the alcohol conversion were not clear. Understanding the mechanisms and identifying the active sites of these reactions can help solve this problem. Detailed investigations of copper-containing catalysts of methanol synthesis and the water-gas-shift reaction (11–22) have been reported over the past 20 years, which have shown the presence of different copper sites on the surface of copper catalysts. In contrast very few studies have been devoted to an elucidation of the mechanism of the cyclohexanol dehydrogenation in an attempt to connect the activity of copper-containing catalysts with the oxidation state of surface copper (3, 23–26). Sivaraj *et al.* (23) have studied Cu–Zn–Al catalysts prepared by a deposition-precipitation method in the reaction of cyclohexanol dehydrogenation. They have

[1] To whom correspondence should be addressed at 110-20 73Rd. Apt. 2M, Forest Hills, NY 11375. E-mail: vfridman@sprintmail.com.

[2] Present address: Benedum Engineering Hall, Department of Chemical and Petroleum Engineering, University of Pittsburgh, Pittsburgh, PA 15261. E-mail: davydov@pitt.edu.

0021-9517/00 $35.00

determined the direct correlation of catalyst activity and the amount of reversible carbon monoxide uptake with a maximum at 30 at.% Cu loading. The authors concluded that metallic copper species are the active sites for the dehydrogenation activity of the copper catalysts. In our opinion, the conclusion of the authors (23) that metallic copper is an active site for the reaction of dehydrogenation of cyclohexanol is not complete. Our analysis of this results showed that these investigators (23) have not considered the previous studies (11–22), nor their own (25), where it was determined that Cu–Zn–Al catalysts with a 30 at.% copper loading have not only a maximum amount of reversible carbon monoxide uptake but also a maximum amount of irreversible adsorbed carbon monoxide. It should be noted that the results of the later study (25) are in a good agreement with results of the earlier studies (21, 22). It is well known that irreversible adsorption of carbon monoxide is directly proportional to the amount of monovalent copper on the catalyst surface (27). The observed (23) maximum of activity at 30% copper is, therefore, not only because of zerovalent copper sites but also because of monovalent copper sites. In our previous studies of the cyclohexanol dehydrogenation reaction (3, 26) the catalysts that had the highest probability for monovalent copper on the surface were more active than catalysts without monovalent copper. On the basis of these (3, 26) and other reported studies (14, 15, 21, 22), we have proposed that copper-containing catalysts have two types of active sites of copper for the reaction of cyclohexanol dehydrogenation.

The present study deals with the surface properties of Cu–Zn, Cu–Zn–Al, and Cu–Mg catalysts with different copper loading with the aim of determining active sites of the reactions of cyclohexanol dehydrogenation and aromatization. The main focus is on changes in the oxidation state of copper and on the dependence of the oxidation state of copper on activity.

EXPERIMENTAL

Catalysts preparation. The Cu–Zn, Cu–Zn–Al, and Cu–Mg catalysts with various atomic compositions were prepared by coprecipitating copper, zinc, aluminum, and magnesium nitrates with a 10% solution of sodium carbonate. Appropriate amounts of $Cu(NO_3)_2 \cdot 3H_2O$, $Zn(NO_3)_2 \cdot 6H_2O$, $Al(NO_3)_3 \cdot 9H_2O$, and $Mg(NO_3)_2 \cdot 6H_2O$ were dissolved in 50 mL of distilled water to obtain 5 g of each catalyst. After the solutions were heated to 80°C, 40 mL of Na_2CO_3 solution was added dropwise over a period of 20 min under vigorous stirring, followed by aging for 1 h at the same temperature. During the aging, the final pH of solution was adjusted to 7.0 by the addition of a small portion of the Na_2CO_3 solution. The precipitate was filtered and suspended in 100 mL of distilled water at 50°C for 10 min, followed by filtration. The washing of the precipitate was repeated four times. The precipitate was dried at 110°C for 16 h to produce the precursor catalyst. The Cu–Zn and Cu–Zn–Al precursor catalysts were finally calcined at 350°C and Cu–Mg precursors were finally calcined at 500°C for 4 h in air. The Cu–Zn, Cu–Zn–Al, and Cu–Mg catalysts were prepared with different copper loadings from pure ZnO, Zn–Al system, and pure MgO up to pure copper oxide. Cu–Zn–Al catalysts were prepared at a constant concentration of aluminium equal to 15 at.%. The compositions of catalysts are presented in Tables 1, 2, and 3.

X-ray diffraction analysis. X-ray diffraction (XRD) analysis of catalysts was carried out using DSOOSIMENS with a copper anode and a nickel filter. The crystallite sizes of metallic copper and copper oxides were estimated from Scherrer's equation (28). These data are summarized in Tables 1, 2, and 3 together with the BET surface areas of the catalysts (N_2 adsorption at 77 K).

Measurements of X-ray photoelectron spectra (XPS). XPS spectra were obtained only for Cu–Zn–Al catalysts before and after reduction and use in the reaction of dehydrogenation of cyclohexanol on an ESCA-3 spectrometer, using AlK_a radiation (1486 eV). The recording was conducted in the range-binding energies from 0 to 1100 eV and then in the spectral region corresponding to the levels Cls, Ols, Cu2$p_{3/2}$, Zn2$p_{3/2}$, Al2s, and Al2p. The C1s-binding energy value of 285 eV has been used as a reference level. The surface composition of atoms in Cu–Zn–Al catalysts was determined on the basis of the peak area intensities of the Cu($2p_{3/2}$)/Zn ($2p_{3/2}$) levels. The relative atomic sensitivity factor used here was obtained from the experimental values of Wagner *et al.* (29) (Cu(2p3/2)/Zn (2p3/2) = 0.88). The reduced Cu–Zn–Al catalysts were transferred to a nitrogen-filled box attached to spectrometer without exposure to air.

Catalytic activity. The activity of catalysts was studied in a continuous flow-type reactor with a fluidized layer of catalyst at 250 and 300°C of flow rates in the range of 0.5–4.0 h. Initially the samples were reduced by mixture (3% H_2 and N_2) at 250°C for 16 h. Reduction times were always three times the time necessary for stoichiometric reduction of CuO to Cu^0. The comparison of the catalysts activities in the cyclohexanol dehydrogenation reaction to cyclohexanone (Reaction 1) was made at the same temperature (250°C) at different reactant space velocities, and at the same conversion of alcohol (=30%), the comparison of the catalysts activities in the cyclohexanol aromatization reaction to phenol (Reaction 2) was made at the same temperature (300°C) and also at different reactant space velocities at the same phenol yield (2.5%).

IR spectroscopy. IR spectroscopy of adsorbed probe molecules (30, 31) has been used to determine the oxidation state of the copper sites. IR spectra of adsorbed species were recorded in the temperature range from 25 to 300°C with an infrared spectrometer (UR-20). The catalysts were

placed in a cell and subjected to exposure to a gaseous mixture of varying compositions at different temperatures. The recording of spectra was performed with compensation of the gas phase. The details of this method have been described in (30). To estimate the state of copper oxidation, two criteria were used, namely, the value of ν CO vibration and thermal stability of the CO complexes with the copper cation. It is known (31, 32) that in the spectra of CO adsorbed on the copper cations the values of ν CO depend on the charge and the structure of the nearer environment of copper (Cu^0–CO <2100 cm^{-1}, Cu^{1+}–CO between 2110 and 2140 cm^{-1}, Cu^{2+}–CO >2140 cm^{-1}) and different thermal stabilities of the complexes (Cu^0–CO is easily destroyed at the temperature range 25–100°C and while the Cu^{1+}–CO is a stable complex, it cannot be destroyed even at 100°C (31).

RESULTS

Catalysts Characterization

Cu-Mg catalysts. A series of copper–magnesium catalysts with final compositions ranging from pure magnesium oxide to pure copper oxide were prepared. X-ray analysis showed a mixture of CuO and MgO was obtained after calcination (Table 1). Even the Cu–Mg catalyst with 10 at.% copper loading (that is equal to 20 wt%) after calcination has in the bulk a trace amount of CuO, and as follows from (33) the rest part of copper is in the solid solution of copper in MgO. The increase of copper loading leads to enhancement of the intensity of the peaks of CuO in X-ray diffraction patterns. After reduction of Cu–Mg catalysts in an atmosphere of hydrogen, the peaks of copper oxides disappeared and the peaks of metallic copper appeared even in catalysts with 10% copper loading (Table 1). The crystallite size of metallic copper after reduction in Cu–Mg catalysts remained almost the same independent of copper loading up to 80%. The size of these crystallites has been increased significantly (Table 1) in Cu–Mg catalysts with copper loading equal to 80% and larger.

TABLE 1

Properties of the Cu–Mg Catalysts before and after Use in the Reaction of Dehydrogenation of Cyclohexanol

Number of catalyst	Catalyst composition (Cu/Mg) (at.%)	BET surface area (m^2/g)	Phase composition; XRD		Cu crystallite size (nm) $d = 0.2088$
			Fresh	After work	
1	10.0/90.0	137.0	MgO, CuO	MgO, Cu	12.7
2	25.0/75.0	121.0	MgO, CuO	MgO, Cu	10.4
3	35.0/65.0	97.0	MgO, CuO	MgO, Cu	11.9
4	52.0/48.0	89.0	MgO, CuO	MgO, Cu	11.7
5	70.0/25.0	69.0	MgO, CuO	MgO, Cu	13.9
6	80.0/20.0	53.0	CuO	Cu	21.6
7	100	15.0	CuO	Cu	31.5

TABLE 2

Properties of the Cu–Zn Catalysts before and after Use in the Reaction of Dehydrogenation of Cyclohexanol

Number of catalyst	Catalyst composition (Cu/Zn) (at.%)	BET surface area (m^2/g)	Phase composition; XRD		Cu crystallite size (nm) $d = 0.2088$
			Fresh	After work	
1	8.0/92.0	67.0	ZnO	ZnO	—
2	20.0/80.0	73.0	ZnO	ZnO	—
3	30.0/70.0	68.0	ZnO, CuO	ZnO, Cu	12.9
4	50.0/50.0	59.0	ZnO, CuO	ZnO, Cu	12.4
5	70.0/30.0	61.0	ZnO, CuO	ZnO, Cu	18.9
6	80.0/20.0	54.0	CuO	Cu	24.6
7	100	15.0	CuO	Cu	31.5

IR-spectra of carbon monoxide adsorbed on Cu–Mg catalysts, which were taken after 10 min of exposure of the catalysts with copper loadings of 10, 25, and 52% to 50 Torr CO at 25°C, are presented on Fig. 1. For catalyst with 10% copper, a single symmetric band is observed centered at 2080 cm^{-1} after reduction in an atmosphere of H_2 (Fig. 1A, a). An evacuation of this catalyst at 25°C for 3 h resulted in disappearance of this band (Fig. 1A, a, dotted lines). The similar dependence was observed for the catalyst with 25% copper loading (Fig. 1A, b). Adsorption of CO on the sample with 52% Cu (spectrum c) resulted in a shift of the band position to 2090 cm^{-1} and an appearance of a small shoulder at 2140 cm^{-1}. Subsequent evacuation of this sample led to disappearance of the band at 2090 cm^{-1} (Fig. 1A, c). According to (31, 32) the positions of this band, maximum and thermal stability of adsorbed CO with cations are characteristics of lineraly adsorbed CO on metallic copper (Cu^0).

Cu-Zn catalyst. The XRD data of the fresh and reduced Cu–Zn catalysts presented in Table 2 indicate the dependence of the bulk phase composition on copper loading, and that X-ray diffraction patterns of Cu–Zn catalysts up to 20% do not display any peaks of CuO in fresh samples nor metallic copper peaks in reduced samples (Table 2). Only the ZnO phase was observed in catalysts equal to 20% copper and less. Based on these results and the conclusions of Klier *et al.* (14, 15) we can assume that a large part of copper in these samples exists in the solid solution of copper in ZnO. X-ray analysis showed a mixture of CuO and ZnO which was obtained after calcination of catalysts with copper equal to 30% and more. After reduction of these catalysts in an atmosphere of H_2 at 250°C, copper oxide reduces to metallic copper (Table 2). As for Cu–Mg, the increase of copper loading in the Cu–Zn catalysts leads to enhancement of the amount of the CuO phase. The size crystallites of metallic copper after reduction of the Cu–Zn catalysts remained almost the same independent of copper loading up to 70%. The size of these crystallites increased significantly (Table 2) in the Cu–Zn catalysts with copper

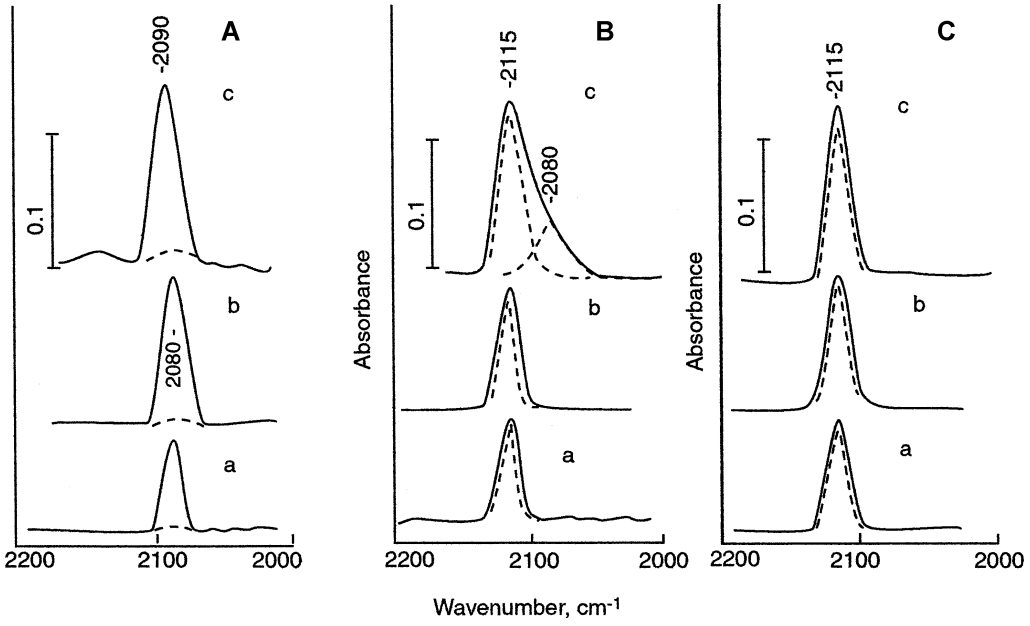

FIG. 1. IR spectra adsorbed CO on the surface Cu–Mg, Cu–Zn, and Cu–Zn–Al catalysts with different Cu loading. (A) IR spectra adsorbed CO at 25°C on the surface of Cu–Mg catalyst after reduction by H_2 at 250°C for 5 h, followed by evacuation at 250°C for 3 h: (a) 10% Cu at.; (dotted line) sample a after evacuation at 25°C for 1 h; (b) 25% Cu at.; (dotted line) sample b after evacuation at 25°C for 1 h; (c) 52% Cu at.; (dotted line) sample c after evacuation at 25°C for 1 h. (B) IR spectra adsorbed CO at 25°C on the surface of Cu–Zn catalyst after reduction by H_2 at 250°C for 5 h, followed by evacuation at 250°C for 3 h: (a) 8% Cu at.; (dotted line) sample a after evacuation at 25°C for 1 h; (b) 20% Cu at.; (dotted line) sample b after evacuation at 25°C for 1 h; (c) 30% Cu at.; (dotted line) sample c after evacuation at 25°C for 1 h. (C) IR spectra adsorbed CO at 25°C on the surface of Cu–Zn–Al catalyst after reduction by H_2 at 250°C for 5 h, followed by evacuation at 250°C for 3 h: (a) 5% Cu at.; (dotted line) sample a after evacuation at 25°C for 1 h; (b) 15% Cu at.; (dotted line) sample b after evacuation at 25°C for 1 h; (c) 20% Cu at.; (dotted line) sample c after evacuation at 25°C for 1 h.

loading equal to 70% and more. This fact suggests a sharp decrease of the dispersion and as result the surface area of copper in these samples.

In contrast to results for the Cu–Mg catalysts, IR spectra of adsorbed CO on reduced Cu–Zn catalysts with 8 and 20% copper displayed symmetric bands centered at 2115 cm^{-1} (Fig. 1B, a and b). Subsequent evacuation of these samples of catalysts at first at 25°C and then at 150°C did not significantly change these spectral features (Fig. 1B, a and b, dotted lines). The position of these band maxima and thermal stability of adsorbed CO are characteristics of linerly adsorbed CO on monovalent copper (Cu^+) (31, 32). Moreover, it can be concluded from this spectrum that first, the copper ions on the surface were homogeneous in the investigated samples, because, according to (39), the surface Cu^+ ions exhibit the formation of two carbonyl complex type, with ν CO 2115 and 2140 cm^{-1}, and secondly, these data testify to the absence of the Cu^{2+} oxide phase (within the sensitivity limits of the method). These results are additional indirect support of our assumption regarding the formation of the solid solution copper with ZnO. Unlike spectra of adsorbed CO on catalysts with 8 and 20% copper, the spectrum of adsorbed CO on catalyst with 30% copper displayed an asymmetric band in the wavenumber range of 2050 to 2140 cm^{-1} centered at 2115 cm^{-1} (Fig. 1B, c). Apparently this spectrum can be resolved into two separate bands centered at 2080 and 2115 cm^{-1}, corresponding to adsorbed CO on metallic Cu and to lineraly adsorbed CO on Cu^+ (31). Evacuation of the sample with 30% copper after adsorption of CO at 25°C resulted in narrowing of the band at 2115 cm^{-1} with the disappearance of low-frequency component (Fig. 1B, c, dotted line). The intensity of the peak centered at 2115 cm^{-1} did not change. These results suggest that copper on the surface of this catalyst exists as monovalent and metallic copper, in agreement with the results and conclusions reported elsewhere (20–22). The catalysts with copper loading more than 30% after reduction in H_2 at 250°C completely lost transparency in the wavenumber range of 2000–2300 cm^{-1}, and IR data of adsorbed CO could not be obtained for these catalysts. It should be noted that the loss of transparency was observed by Boccuzzi *et al.* (34, 35) after reduction of pure ZnO, which was attributed to the formation of donor centers V_O+ (Monoionized oxygen vacancies). Boccuzzi *et al.* have observed that unlike pure ZnO, the reduced binaries in the range of copper loading up to 30% exhibit a good IR transparency. They have concluded that reduction conditions guarantee that sufficient quantities of Cu^{2+} are still present in the ZnO phase as a solid solution of copper in ZnO, at least in the bulk, to prevent the formation of high amounts of V_O+.

Boccuzzi *et al.* have not studied the Cu–Zn catalysts with more than 30% copper. In our investigation we have observed the loss of transparency also for catalysts at 40 and 50% copper. Based on Boccuzzi *et al.*'s explanation we have assumed that in Cu–Zn catalysts, in the loading range greater than 30%, CuO does not form the solid solution of CuO in ZnO. Absence of the solid solution copper in ZnO, which can keep Cu in ZnO even after reduction, leads to the formation of distinct phases of copper and zinc oxides. On the other hand, CuO can be easily reduced to metallic copper. ZnO without soluble Cu^{2+} has a great amount of monoionized oxygen vacancies V_O+, which bring about a complete loss of transparency in the range 2000–2300 cm^{-1} in the IR spectrum of these catalysts.

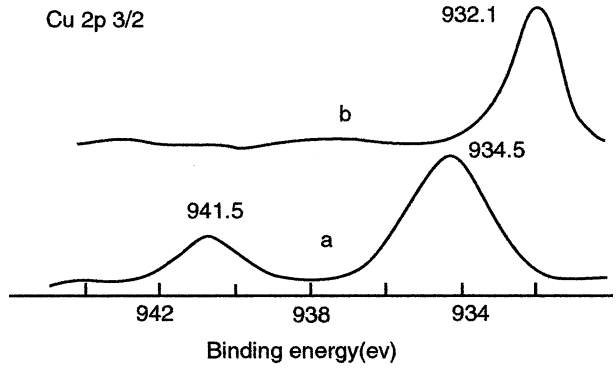

FIG. 2. XPS spectrum of Cu–Zn–Al catalysts (40% Cu at.): (a) after preparation; (b) after reduction by H_2 at 250°C for 5 h.

Cu–Zn–Al catalysts. Cu–Zn–Al catalysts were prepared with different concentrations of Cu and Zn and at the constant concentration of Al equal to 15 at.%. X-ray analysis of the Cu–Zn–Al catalysts with 5, 10, and 15% Cu shows (Table 3) the existence of only ZnO and an absence of peaks from any copper and aluminum-containing compounds. This is due either to the formation of a solid solution of Cu and Al in the lattice of ZnO or to the high dispersion of copper and aluminum amorphous compounds. According to the XRD data (Table 3) Cu–Zn–Al catalysts with copper loading even of 20% after calcination have not exhibited bulk CuO, but after reduction of this catalyst a trace amount of metallic copper was observed in the X-ray diffraction patterns. Calcination of the catalysts with 40% copper and higher led to a mixture of CuO and ZnO (Table 3). The increase of the copper loading led to an increase in the CuO. The diameter of metallic copper crystallites increased significantly (Table 3) in Cu–Zn–Al catalysts with copper loading equal to 80% and more, and this fact is indirect evidence for a significant decrease in the surface area of copper.

The IR spectra of CO adsorbed on the reduced surface of Cu–Zn–Al catalysts with concentrations of 5, 15, and 20% Cu displayed one symmetric band centered at 2110 cm^{-1} for the sample with 5% Cu and at 2115 cm^{-1} for samples with 10 an 15% Cu (Figs. 1C, a, b, and c). The copper ions in these samples were homogeneous and the states of copper ions on the surface of both Cu–Zn and Cu–Zn–Al catalysts were similar. Evacuation of the samples even at 150°C did not change the spectral picture (Figs. 1C, a, b, and c, dotted lines), which is evidence of the high level of thermal stability of adsorbed CO. The position of the band and the characteristic of thermal stability suggest that these bands can be attributed to the stretching mode of CO in Cu^+–CO complexes (31, 32). As for Cu–Zn catalysts, the Cu–Zn–Al catalysts with copper loading equal to and more than 40% completely lost transparency in the wavenumber range 2000–2300 cm^{-1} after reduction in H_2 at 250°C. According to our previous discussion for Cu–Zn this result is probably because of the weak interaction of copper with ZnO in Cu–Zn–Al catalysts with copper equal to 40% and greater.

X-ray photoelectron spectra of the Cu($2p_{3/2}$) level were practically invariant with the catalyst composition. XP spectra of Cu ($2p_{3/2}$) of Cu–Zn–Al catalysts with 15% copper before and after reduction in an atmospheric hydrogen stream are shown in Fig. 2. This spectra indicates a well-separated main peak at 934.5 eV and satellite peak at 941.5 eV, characteristic of Cu^{2+} (Fig. 2a). The satellite peak

TABLE 3

Properties of the Cu–Zn–Al Catalysts before and after Use in the Reaction of Dehydrogenation of Cyclohexanol

Number of catalyst	Catalyst composition (Cu/Zn/Al) (at.%)	BET surface area (m^2/g)	Phase composition; XRD		Cu crystallite size (nm) $d = 0.2088$	Surface ratio of the atom (Cu/Zn); XPS	
			Fresh	After work		Fresh	After work
1	5.0/80.0/15.0	87.0	ZnO	ZnO	—	0.068	0.096
2	15.0/70.0/15.0	77.0	ZnO	ZnO	—	0.170	0.160
3	20.0/65.0/15.0	73.0	ZnO	ZnO, Cu traces	11.2	0.290	0.320
4	40.0/45.0/15.0	79.0	ZnO, CuO traces	ZnO, Cu	13.2	0.625	0.523
5	60.0/25.0/15.0	65.0	ZnO, CuO	ZnO, Cu	14.9	3.545	1.150
6	80.0/5.0/15.0	56.0	CuO	Cu	28.6	10.700	1.983
7	100	15.0	CuO	Cu	31.5		

of Cu($2p_{3/2}$) band characteristic of Cu^{2+} (36) ions disappeared completely after reduction and the binding energy level shifted to a lower energy (932.1 eV), indicating unambiguously the complete reduction of Cu^{2+} to lower valence states (Fig. 2b).

In this work we could not determine the concentration of aluminum on the surface of the Cu–Zn–Al catalysts because of the low intensities Al2p and Al2s lines. This result does not seem surprising, because of the low loading of Al (15 at.% of aluminum corresponds to 6.2 wt%). Similar results have been obtained by other authors (16) for Cu–Zn–Al catalysts with Al loading of 18 and 17 at.%.

Surface compositions derived from XPS intensities are reported in the Table 3. The Cu/Zn ratio as a function of copper loading increases monotonically with an increase in copper catalysts. The comparison of Cu/Zn ratio for calcinated and reduced samples indicates low level stability of copper in catalysts with copper greater than 40% of Cu, since the Cu/Zn ratio after reduction of these catalysts decreased significantly.

Catalyst Activity

Dehydrogenation of cyclohexanol to cyclohexanone. The catalyst activity of Cu–Mg, Cu–Zn, and Cu–Zn–Al catalysts in Reaction 1 is presented as a rate of reaction per gram of catalyst (Fig. 3I) and a rate of the reaction per specific area of catalyst (Fig. 3II). As follows from Fig. 3 the initial MgO, ZnO, and Zn–Al systems do not catalyze cyclohexanol dehydrogenation. The addition of copper to the MgO system leads to a gradual increase in the activity for the synthesis of ketone from alcohol (Fig. 3I, a). The rate of this reaction per unit of the mass for Cu–Mg catalysts achieved a maximum at a copper loading of 52%. The subsequent increase of copper in Cu–Mg catalysts reduced the rate of the reaction of cyclohexanol dehydrogenation (Fig. 3I, a). In contrast to results for Cu–Mg catalysts the addition of even 8% copper to ZnO and 5% to Al-Zn systems resulted in a sharp increase in cyclohexanone synthesis (Fig. 3I, b and c). The maximum rates of this reaction were observed for Cu–Zn catalysts at 30% copper loading and for Cu–Zn–Al catalysts at 20% copper loading. For all systems the minimum rate of the reaction of cyclohexanol dehydrogenation per gram of catalyst was observed for pure metallic copper. It should be noted that the dependence of the rate of Reaction 1 on Cu–Mg and on Cu–Zn-containing catalysts totally differs (Fig. 3I). Similar results were observed for the activity of these catalysts calculated per unit of the catalyst surface (Fig. 3II), and only the position of pure copper is different. The activity of pure copper per square meter is twice than that of catalysts with more than 50% copper loading (Fig. 3II). This observation suggests that the sufficient part of the surface of these catalysts even with 80% copper loading is contributed by the surface of inactive support.

Aromatization of cyclohexanol to phenol. The activities of the catalysts in the cyclohexanol aromatization reaction also has been calculated per unit of the mass and per unit of the specific area of the catalysts (Figs. 4I and 4II). As follows

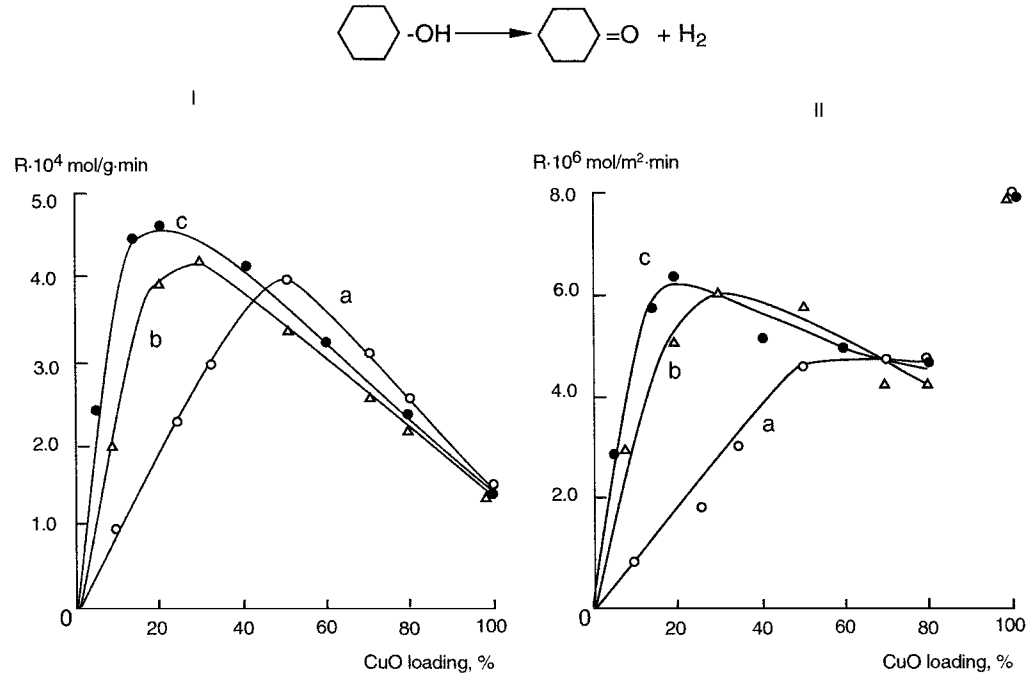

FIG. 3. The rate of the dehydrogenation reaction of cyclohexanol to cyclohexanone per unit of the mass (mol/g × min) (I) and per unit of the specific area (mol/m^2 × min) (II) as a function of copper loading ($T = 250°C$): (a) Cu–Mg catalysts, (b) Cu–Zn catalysts, (c) Cu–Zn–Al catalysts.

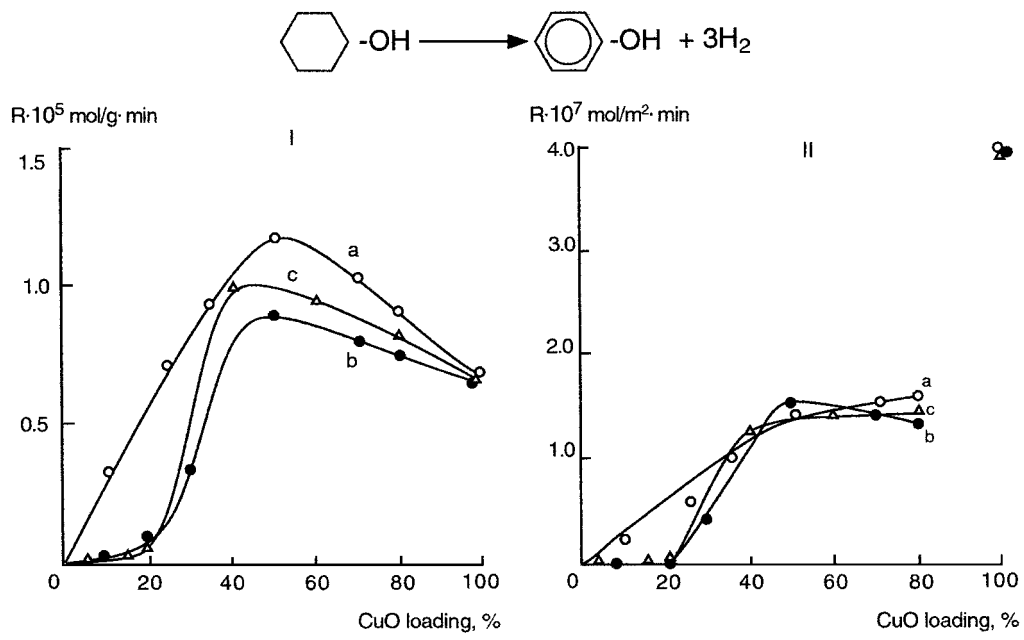

FIG. 4. The rate of the aromatization reaction of cyclohexanol to phenol per unit of the mass (mol/g × min) (I) and per unit of the specific area (mol/m^2 × min) (II) as a function of copper loading ($T = 300^\circ$C): (a) Cu–Mg catalysts, (b) Cu–Zn catalysts, (c) Cu–Zn–Al catalysts.

from these figures the activity of the Cu–Mg catalysts in the cyclohexanol aromatization reaction depends on amount of copper in catalysts (Figs. 4I, a, and 4II, a). Cu–Mg catalysts with 52% Cu showed a maximum in activity per unit of the mass in Reaction 2 (Fig. 4I, a). The increase of copper in Cu–Mg catalysts greater than 52% reduces the rate of the reaction of cyclohexanol aromatization (Fig. 4I, a).

Phenol is not formed on the Cu–Zn and Cu–Zn–Al catalysts with a concentration of copper less than 20% (Fig. 4I,b and c). A very small amount of phenol is formed on the these catalysts with 20% copper. The maximum activity calculated per unit of the catalyst mass for Cu–Zn catalysts in Reaction 2 is observed at 30% copper loading and for Cu–Zn–Al catalysts at 40% copper loading. Pure metallic copper also catalyzes the reaction of aromatization of cyclohexanol to phenol.

Similar results were observed for activity of these catalysts calculated per unit of the catalyst surface (Fig. 4II), particularly for the catalysts with less than 40% copper loading. The activities calculated per unit of the specific area for the all catalyst system, practically, do not change in the range of Cu loading from 40 to 80%. The maximum rate of Reaction 2 per square meter is observed for pure metallic copper (Fig. 4II, a, b and c.).

DISCUSSION

Cu–Zn and Cu–Zn–Al catalysts have been investigated by a gamut of physical techniques, but only a few studies have been devoted to the investigation of Cu–Mg catalysts (33, 37–39). An earlier attempt to correlate the activity with the surface structure of Cu–Mg catalysts led to the identification of isolated Cu^{2+} ions in open octahedral holes and evidence of the migration of isolated copper ions to form metallic clusters (33). Detailed ESR and UV spectroscopic studies (37) have shown the presence of isolated and strongly associated Cu^{2+} ions in initial samples. The results of the present investigation have shown that in catalyst with 10% copper only a very small amount of CuO is observed after calcination. Apparently the remaining copper is either in an X-ray amorphous phase or in a solid solution CuO in MgO (39). However, after reduction, even in catalyst with 10% copper loading, both isolated ions Cu^{2+} in a solid solution of MgO and strongly associated Cu^{2+} were reduced to metallic copper in an atmosphere of hydrogen at 250°C (Table 1). We have considered the possibility that with Cu–Mg catalysts, the solid solution of copper in MgO could be reduced also to monovalent copper, as in the case with the Cu–Zn catalysts (14, 15), at least in catalysts with a low loading of copper where the formation of the solid solution of copper in a support is most probable. The results of IR spectroscopy of adsorbed CO have shown that copper is reduced to a metallic state independently of the composition of Cu–Mg catalysts. Apparently, the magnesium oxide does not have the ability to inhibit the complete reduction of copper oxide to the metallic state in contrast to ZnO (15). The possible lowering of the effective charge of copper ions under the specific influence of basic magnesium oxide has been attributed to the presence of electron-donor ligands in the coordination sphere of a cation (31). The difference in electron-donor ability between MgO and ZnO accounts for the difference in the influence of these

supports for the reduction of copper. Thus, copper on the reduced surface of all Cu–Mg catalysts exists only in the oxidation state Cu^0, and the copper loading influences only a number of the metallic copper atoms and active sites on the surface. Actually, these results and activity data for the Cu–Mg catalysts strongly support zerovalent copper as an active site of the dehydrogenation of cyclohexanol. Considerable attention to the study of Cu–Zn and Cu–Zn–Al catalysts (11–22) was mostly due to the practical importance of using these catalysts for the synthesis of methanol. One of the first investigations of these catalysts was performed by Herman *et al.* (14) and Menta *et al.* (15). The compositional profile of calcined Cu–Zn catalysts, determined by X-ray diffraction (14), showed that a part of copper is in the solid solution of CuO in ZnO. According to X-ray microanalysis (15) up to 6% of copper after calcination exists in the solid solution. Consequently, after reduction of the oxides, fine dispersions of metallic copper appear in the 10–30% copper catalysts. Herman *et al.* (14) have shown that the reduction of catalysts leads to an increase in the amount of the solid solution of monovalent copper in the lattice of ZnO. Authors (14, 15) have explained that dissolution Cu^+ in ZnO is much more favorable than Cu^{2+} because Cu^+ is isoelectronic with Zn^{2+}. The limited solubility of Cu^+ in ZnO is based on the requirement of electroneutrality, either by oxygen vacancies or by intersticial cations, upon substitution of some Zn^{2+} by Cu^+ (14). The catalysts with a composition close to 30/70 are characterized as a complex of two forms of copper, one appearing in and strongly interacting with the zinc oxide phase (solid solution of Cu^+ in ZnO) and the other being a fine copper metal dispersion (14, 15). The Herman-Klier model of copper-zinc-contained catalysts has been accepted by many researchers to understand their own results on these catalysts. Later Klier *et al.* (40) estimated that the average copper concentration of 15% as a solid solution in the ZnO phase is present in a 30/70 catalyst (50% of total Cu amount); they considered this number a limit of Cu solubility in ZnO. Similar results have been obtained by Okamoto *et al.* (21, 22), who found that two distinct types of Cu metal species were formed on the catalyst surface, and their proportions depend on the catalyst composition. In high Cu content catalysts (>25 wt% CuO), Cu metal particles are predominant, whereas in the low Cu content catalysts (<10 wt% CuO), a Cu metal species, which is best characterized by two-dimensional epitaxial monolayer over ZnO, is predominant. It was concluded that Cu metal particles with charge Cu^0 on the surface are formed mainly from crystalline and an amorphous copper oxide phase, while two-dimensional Cu species Cu^0–Cu^+ including Cu^+ are derived from the Cu^{2+} dissolved in the ZnO lattice (22). Gasbassi and petrini (16, 17) obtained results which showed the formation of the solid solution of CuO in the lattice of ZnO in low content Cu–Zn catalysts. Concurrently, Yur'eva *et al.* (41–43) studied the mechanisms of stages in the preparation of Cu–Zn and Cu–Zn–Al catalysts. Based on the conclusions of previous studies, they found a way to increase the solubility of copper in ZnO by anion modification to enhance the amount of defects in the lattice of ZnO (44–46). A solid solution of copper ions in zinc oxide modified with anions was established as an oxide precursor of the active state (18). In the one of these studies (47), Plasova *et al.* showed that the reduction of a solid solution of Cu in ZnO carries out through the formation phase of metallic copper which very easily vanishes when the H_2 atmosphere is replaced with He. They have explained this observation by the formation of a complex proton-stabilized system of ZnO modified by anions with epitaxially bonded copper species $[Cu_x^0 - H_{2x}^+ Cu_{0.1-x}^{2+} Zn_{0.9}O]$ (47).

The compositional profile of Cu–Zn and Cu–Zn–Al catalysts investigated in the present study shows that in low content catalysts, copper exists either in an amorphous state or in the solid solution of CuO in the lattice of ZnO (no CuO phase was found for copper loading to 20% for Cu–Zn–Al and Cu–Zn catalysts), and that only in catalyst with 20% after reduction, traces of metallic copper have been found. Based on the IR spectroscopy data of the present study showing that the main oxidation state of copper on the surface of low content Cu–Zn and Cu–Zn–Al catalysts is Cu^+ (Fig. 2) and conclusions of the Klier *et al.* studies (14, 15), we propose that only a small part (an negligible amount) of copper in these catalysts is amorphous copper oxide. The majority of copper in these catalysts is in the solid solution of copper in ZnO. The increase of copper loading in catalysts leads to the reduction in the amount of ZnO in the system and to the decrease of ZnO, which is able to accept copper with the formation of the solid solution. Consequently, copper in Cu–Zn and Cu–Zn–Al catalysts with Cu greater than 20% forms a distinct phases of copper oxide, which coexists with the solid solution of copper in ZnO. Although we did not determine the oxidation state of copper on the surface of Cu–Zn and Cu–Zn–Al catalysts with copper greater than 30 and 20%, respectively, because of the loss of IR transparency, we have no doubt concerning the oxidation state of copper on the surface of these catalysts. Since Cu^0 is the most thermodynamically beneficial state of copper for the CuO reduction by hydrogen at 250°C (our own thermodynamic calculations), we propose that the main oxidation state of copper in these samples is Cu^0. This confirmation is supported by indirect evidence from XRD, XPS data of the present investigation, and conclusions of the different investigators, who have studied Cu–Zn and Cu–Zn–Al catalysts by Auger electron spectroscopy (22) and IR spectroscopy (48). Thus, in the case where the copper oxide does not have any inhibiting influence of other components for the reduction of CuO, there is no possibility for the formation of copper in the oxidation state another than metallic copper. Based on the limit of the solubility of copper in ZnO proposed by Dominiquez *et al.*

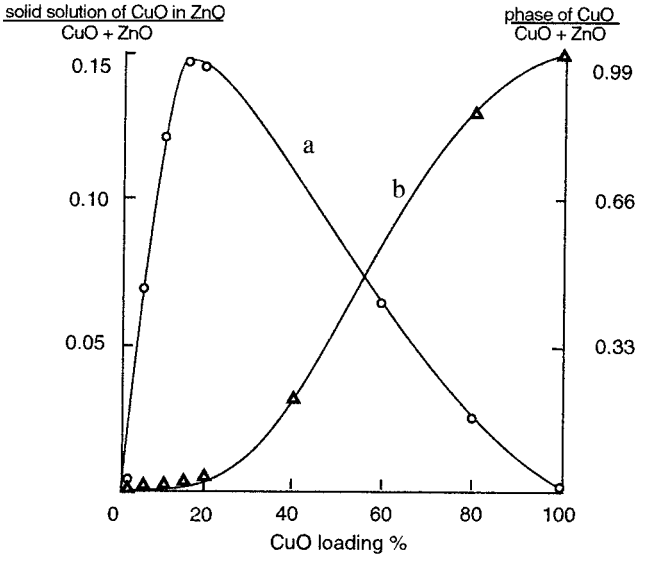

FIG. 5. Assumable phase composition of Cu–Zn catalyst, calculated based on the Herman-Klier model of solubility of copper in ZnO in Cu–Zn catalysts: (a) solid solution of copper in ZnO; (b) phase of CuO.

(40) and the assumption that the conditions of the preparation of catalysts provide the formation of solid solution of Cu in ZnO equal to the limit solubility we have calculated the assumable phase composition (concentrations of the solid solution of copper in ZnO and distinct phase of CuO) of Cu–Zn and Cu–Zn–Al catalysts as a function of Cu/Cu + Zn ratio (Fig. 5). It should be noted that results of our calculation of the phase composition Cu–Zn catalysts are in very good agreement with those of Okamoto *et al.* (21) and our X-ray data (Table 3). According to this calculation, the amount of the solid solution of copper in ZnO at first increases sharply up to 15% (Fig. 5a) and then gradually decreases with an increase of the copper content greater than 20–30%. Comparisons of the calculated phase composition (Fig. 5, a) and the activity of Cu–Zn and Cu–Zn–Al catalysts (Fig. 3I, b and c) as a function of copper are parallel to each other. These data indicate that the solid solution of Cu in lattice of ZnO is a precursor of at least one kind of active site for cyclohexanol dehydrogenation to cyclohexanone. On the other hand, the comparison of the calculated amount of the CuO phase (Fig. 5, b) and the rate of Reaction 2 (Fig. 4I, b and c) with the composition of these catalysts indicates that the formation of phenol begins after the appearance of the distinct CuO phase in Cu–Zn and Cu–Zn–Al catalysts. This result suggests that the amorphous and crystal phases of CuO are precursors of the active sites for the reaction of aromatization of cyclohexanol to phenol. Since Cu–Zn-containing catalysts with low Cu loading have on their surface only copper in the Cu^+ oxidation state, and they do not form phenol from cyclohexanol, we concluded that monovalent copper sites are not able to catalyze the aromatization reaction.

Finally, we concluded that copper-containing catalysts of dehydrogenation of cyclohexanol have on the surface two kinds of active copper sites for Reaction 1 such as monovalent copper (Cu^+) and zerovalent copper (Cu^0), which work independently. The ratio between these sites depends on the composition and conditions of catalyst preparation. The Cu–Mg catalysts do not have sites of monovalent copper, and the activity of these catalysts is a function of the metallic copper surface. The increase of the activity in the cyclohexanol dehydrogenation reaction to cyclohexanone of Cu–Mg catalyst happens with enhancement of copper loading and the surface metallic copper in catalysts to attain the maximum, and a subsequent decrease of the rate is attributed to a reduced dispersion and surface area of metallic copper.

In the case of copper-zinc-containing catalysts in the low Cu content range, the increase in copper loading leads to an increase in the amount of the solid solution of Cu in ZnO, and, as result, to an increase of both the amount of monovalent copper sites and the activity of catalysts. Beginning from 15% composition and greater the enhanced catalyst activity results in the formation of both kinds of copper active sites: monovalent copper and fine dispersion metallic copper. Monovalent copper is the predominant active site in copper-zinc-containing catalysts up to 20–30%. Beginning at 15–20% copper the activity of the catalysts in this range changes insignificantly, probably because the small reduction of the amount of monovalent copper sites is substituted by the formation of a large number of metallic copper sites (for instance, 20 and 40% Cu–Zn–Al catalyst Fig. 3I, c). It is likely that the catalysts with 60% copper and greater do not have monovalent copper on the surface at all, and the activity of these catalysts is a function only of the copper surface area. The shift of the maximum activity of copper-zinc-containing catalysts toward the low Cu content range suggests that the activity of single site monovalent copper is higher than the activity of single site zerovalent copper.

The dependence rate of the aromatization reaction of cyclohexanol indicates that phenol is not formed on copper-zinc-containing catalysts with copper less than 20%. This observation is evidence that monovalent copper sites are not the active sites of the reaction of the phenol formation. The formation of phenol is observed only after the appearance of metallic copper. The rate of Reaction 2 attains the maximum at a copper content of 40% for Cu–Zn–Al catalysts and the subsequent increase of copper leads to a slowly decreasing rate of Reaction 2. The reason for this decrease on catalysts with 60% Cu is the decrease of the dispersion and the surface area of copper. It should be noted that for Cu–Mg catalysts the dependencies of rates of Reaction 1 and Reaction 2 on composition are parallel, and this fact is additional evidence that in these catalysts both reactions occur via the same active sites.

To compare the activities of monovalent and zerovalent copper sites the activity data for pure metallic copper and for Cu–Zn–Al catalyst with 5% Cu have been used, since there is apparently only one kind of copper site on each of them (monovalent copper on the surface of 5% Cu–Zn–Al catalyst and zerovalent copper on the surface of reduced CuO). The catalysts of middle compositions were not used because of a higher probability for the existence of two kinds of copper sites on the surface of these catalysts.

Several techniques have been developed and applied for the evaluation of the specific metal surface of copper catalysts, such as chemisorption of carbon monoxide (49, 50), hydrogen (51), and oxygen (52) and decomposition of nitrous oxide (53). In a recent study Dandekar and Vannice have used the combined approach with irreversible CO adsorption and N_2O decomposition measurements (54, 55) for determination of the dispersion of supported Cu catalysts. The crystallite sizes obtained from these estimates were compared to those obtained from TEM and XRD measurements and were found to be in very good agreement (54). In our investigation we have used the values of the total specific surface, obtained by BET, as well as the ratio between atoms on the surface, obtained by XPS. BET has been used by Herman *et al.* (14) and Okamoto *et al.* (21) to estimate the surface of reduced CuO.

According to XPS data the Cu–Zn–Al catalysts have on the surface only atoms of Cu and Zn and the surface concentration of Al is equal to zero (Table 3). On the other hand, monovalent copper in catalysts with 5% copper exists on the surface and in the bulk in only the solid solution of Cu^+ in ZnO. The observation that monovalent copper substitutes zinc in lattice ZnO manifests the correctness of the simplification that one atom of Cu^+ and one atom of Zn^{2+} in lattice of ZnO form equal surface areas since they have exactly the same crystal structure and surrounding. The results of calculations have shown that the copper surface areas in the 5% Cu–Zn–Al catalyst and pure metallic copper are equal to 5.7 and 11.7 m^2/g, respectively. The numbers of monovalent and zerovalent sites were obtained based on the values of the copper surface areas of these catalysts and assumptions of a Cu^+ site density of 5.2×10^{18} m^{-2} (56) and of a Cu^0 site density of 1.4×10^{19} m^{-2} (57). Activities as well as turnover frequencies for $Cu^+ = 1.2$ s^{-1} and $Cu^0 = 0.086$ s^{-1} sites have been calculated. The result indicates that the activity of the Cu^+ site is 14 times greater that of than Cu^0.

CONCLUSIONS

The X-ray diffraction, X-ray photoelectron spectroscopy, IR spectroscopy of chemisorbed carbon monoxide and kinetic data have been employed to determine the active sites of the reaction of dehydrogenation of cyclohexanol to cyclohexanone and the reaction of aromatization of cyclohexanol to phenol. Two kinds of copper active sites of the reaction of cyclohexanol dehydrogenation to cyclohexanone have been revealed (monovalent copper and metallic copper), and it was shown that the sites of monovalent copper are significantly more active than the sites of metallic copper. Moreover, the sites of monovalent copper are selective, and they do not catalyze the reaction of the phenol formation. At the same time, the sites of metallic copper are active sites not only for the reaction of dehydrogenation of alcohol to ketone but also for the reaction of aromatization of cyclohexanol to phenol; therefore, these sites are not selective.

ACKNOWLEDGMENT

The authors are grateful to Professor T. Yur'eva (Boreskov's Institute of Catalysis, Novosibirsk, Russia) for consultations concerning the methods of catalyst preparation.

REFERENCES

1. Bedina, L. N., Polovkina, T. S., Fridman, V. Z., and Voronkova, O. N., *Chem. Ind.* (in Russian) **9**, 5 (1987).
2. Zadymov, V. V., Smirnov, I. V., and Topchieva, K. V., *J. Phys. Chem.* (in Russian) **54**, 711 (1980).
3. Fridman, V. Z., Bedina, L. N., and Petrov, I. Y., *Kinet. Catal.* (in Russian) **29**, 621 (1988).
4. Kozlov, N. S., Mostovai, L. I., Sedel'zeva, M. A., and Gypalo, V. I., *Kinet. Catal.* (in Russian) **27**, 244 (1986).
5. Nikiforova, N. N., and Gavrenko, K. A., *Petrochemistry* (in Russian) **14**, 116 (1974).
6. Orizarsky, I. V., Petrov, L. A., and Petrova, V. M., *React. Kinet. Catal. Lett.* **17**, 427 (1981).
7. Chang, H. F., and Saleque, M. A., *Appl. Catal. A* **103**, 233 (1993).
8. Jeon, G. S., and Chung, J. S., *Appl. Catal.* **115**, 29 (1994).
9. Chen, W. S., and Lee, M. D., *Appl. Catal.* **83**, 201 (1992).
10. Chang, H. F., Saleque, M. A., Hsu, W. S., and Lin, W. H., *J. Mol. Catal.* **109**, 249 (1996).
11. Monnier, J. R., Hanrahen, M. J., and Apai, G., *J. Catal.* **92**, 119 (1985).
12. Shimomura, K., Ogawa, K., Ora, M., and Kotera, M., *J. Catal.* **52**, 191 (1978).
13. Fleisch, T. H., and Mievilie, R. L., *J. Catal.* **90**, 165 (1984).
14. Herman, R. G., Klier, K., Simmons, G. W., Finn, B. P., and Bulko, J. B., *J. Catal.* **56**, 407 (1979).
15. Menta, S., Simmons, G. W., Klier, K., and Herman, R. G., *J. Catal.* **57**, 339 (1979).
16. Garbassi, F., and Petrini, G., *J. Catal.* **90**, 106 (1984).
17. Petrini, G., and Garbassi, F., *J. Catal.* **90**, 113 (1984).
18. Bailie, J. E., Rochester, C. H., and Millar, G. J., *Catal. Lett.* **31**, 333 (1995).
19. Plyasova, L. M., Yur'eva, T. M., Kriger, T. A., Makarova, O. V., Zaikovskii, V. I., Solov'eva, L. P., and Shmakov, A. N., *Kinet. Catal.* (in Russian) **36**, 464 (1995).
20. Chiotti, G., and Boccuzzi, F., *Catal. Rev.-Sci. Eng.* **29**, 151 (1987).
21. Okamoto, Y., Fukino, K., Imanaka, T., and Teranlchi, S., *J. Phys. Chem.* **87**, 3740 (1983).
22. Okamoto, Y., Fukino, K., Imanaka, T., and Teranlchi, S., *J. Phys. Chem.* **87**, 3747 (1983).
23. Sivaraj, C., Reddy, B. M., and Rao, P. K., *Appl. Catal.* **45**, L11 (1988).
24. Sivaraj, C., Srinivas, S. T., Rao, V. N., and Rao, P. K., *J. Mol. Catal.* **60**, L23 (1990).
25. Sivaraj, C., Reddy, B. M., and Rao, P. K., *J. Mol. Catal.* **47**, 17 (1988).

26. Fridman, V. Z., Michal'chenko, E. D., Tryasunov, B. G., Ziborov, A. V., and Plyasova, L. M., *Kinet. Catal.* (in Russian) **32**, 922 (1991).
27. Parris, G. E., and Klier, K., *J. Catal.* **97**, 374 (1986).
28. Cullity, B. D., "Elements of X-Ray Diffraction." Addison-Wesley, Reading, MA, 1956.
29. Wagner, C. D., Davis, L. E., Zeller, M. V., Taylor, J. A., and Raymood, R. H., *Surf. Interface Anal.* **3**, 211 (1981).
30. Shecochihin, U. M., and Davydov, A. A., "Methodics of IR Studies in Physicochemistry of Semiconductor Surface (VINITY)," N. 5014-83, pp. 1–110. Moscow, 1983.
31. Davydov, A. A., "Infrared Spectroscopy of Adsorbed Species on the Surface of Transition Metal Oxides." (Chichester), New York, 1990.
32. Gallardo Amores, J. M., Sanchez Estribano, V., Busca, G., and Loreazelli, V. J., *J. Mater. Chem*. **4**, 965 (1994).
33. Maksimov, N. G., Chigrina, V. A., Boreskov, G. K., Anufrienko, V. F., and Yur'eva, T. M., *Kinet. Catal.* (in Russian) **13**, 446 (1972).
34. Boccuzzi, F., Ghiotti, G., and Chiorino, A., *J. Chem. Soc., Faraday Trans.* **79**, 1779 (1983).
35. Boccuzzi, F., Morterra, C., Scala, R., and Zecchina, J., *J. Chem. Soc., Faraday Trans.* **77**, 2059 (1981).
36. Shinkarenko, V. G., and Anufrienko, V. F., *Theor. Exp. Chem*. (in Russian) **12**, 270 (1976).
37. Boudart, M., Derouane, E. G., Indovina, V., and Walters, A. B., *J. Catal.* **39**, 115 (1975).
38. Davydov, A. A., Rubene, N. A., and Budneva, A. A., *Kinet. Catal.* (in Russian) **19**, 969 (1978).
39. Davydov, A. A., Prudnikova, O. Yu., and Yur'eva, T. M., *Kinet. Catal.* (in Russian) **30**, 477 (1989).
40. Dominiquez, J. M., Simmons, G. W., and Klier, K., *J. Mol. Catal.* **20**, 369 (1983).
41. Yur'eva, T. M., and Minyukova, T. P., *React. Kinet. Catal. Lett.* **29**, 55 (1985).
42. Kuznetsova, L. I., Yur'eva, T. M., and Minyukova, T. P., *React. Kinet. Catal. Lett.* **19**, 355 (1982).
43. Yur'eva, T. M., *Kinet. Catal.* (in Russian) **26**, 686 (1985).
44. Ketchik, S. V., Yur'eva, T. M., and Plysova, L. M., *Izv. Sib. Otd. Akad. Nauk. USSR* (in Russian) **6**, 109 (1983).
45. Ketchik, S. V., Yur'eva, T. M., and Plysova, L. M., *Izv. Sib. Otd. Akad. Nauk. USSR* (in Russian) **1**, 36 (1984).
46. Ketchik, S. V., Yur'eva, T. M., and Plysova, L. M., *Izv. Sib. Otd. Akad. Nauk. USSR* (in Russian) **4**, 37 (1984).
47. Plysova, L. M., Yur'eva, T. M., Kriger, T. A., Makarova, O. V., Zaikovskii, V. I., Solov'eva, L. P., and Schmakov, A. N., *Kinet. Catal.* (in Russian) **36**, 425 (1995).
48. Bailey, S., Froment, G. F., Snoeck, J. W., and Waugh, K. C., *Catal. Lett.* **30**, 99 (1995).
49. Cormach, D., and Moss, R. L., *J. Catal.* **13**, 1 (1969).
50. Smith, J. S., Thrower, P. A., and Vannice, M. A., *J. Catal.* **68**, 270 (1981).
51. Spenadel, L., and Boudart, J., *J. Phys. Chem*. **64**, 205 (1960).
52. Vasilevich, A. A., Shapiro, G. P., Alekseev, A. M., Semenova, T. A., Markina, M. I., Vasileva, T. A., and Budkina, O. G., *Kinet. Catal.* (in Russian) **16**, 1363 (1975).
53. Dvorak, G., and Pasek, J., *J. Catal.* **18**, 108 (1970).
54. Dandekar, A., and Vannice, M. A., *J. Catal.* **178**, 621 (1998).
55. Dandekar, A., Baker, T. K., and Vannice, M. A., *J. Catal.* **183**, 131 (1999).
56. Kington, G. L., and Holmes, J. M., *Trans. Faraday Soc.* **49**, 417 (1953).